FCS and noticeable for RICS and msICS. We could confirm the influence of saturation with FCS measurements of the Alexa488 solution where the diffusion correlation time and the derived focal radius increased with increasing illumination power, see Fig. 2a.

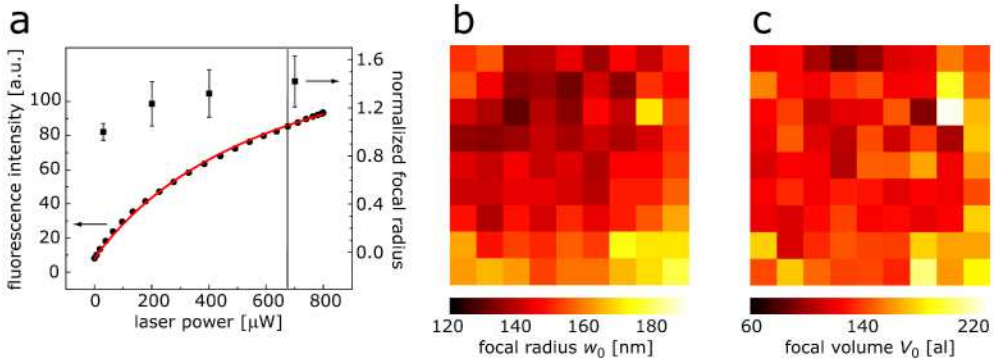

Fig. 2. Characterization of the PSF. (a) Mean fluorescence intensity of Alexa488 taken from confocal images (circles, left axis) and the fit of Eq. (7) (red line) as well as the focal radius normalized to the value determined at 30 μW (squares, right axis) as a function of incident laser intensity. The vertical line marks the saturation power. (b) Map of the focal radius w_0 and (c) of the focal volume V_0 as determined with FCS of Alexa488 in solution on a 9 × 9 array of points covering an area of 243 × 243 μm^2. The variations are very small within the central 135 × 135 μm^2 area where the experiments were carried out.

To ensure that the focal volume of the laser beam is sufficiently homogenous throughout the field of view (FOV) and does not affect the resulting diffusion coefficient, we generated a map of 9×9 FCS point measurements of 20 nM Alexa 488 (5×60 s each) yielding the characteristic diffusion correlation time τ_{diff} and structure parameter κ. Using $D_{Alexa,\ 20°C} = 210$ μm^2 s^{-1} [35], distribution maps of the lateral focal radius w_0 in μm and the focal volume V_0 in μm^3 or fl, respectively, were obtained, see Fig. 2b, c. Average values for w_0 and V_0 are 0.140±0.003 μm and 0.126±0.017 fl, respectively, for the central 3×3 array of 81×81 μm^2 and 0.141±0.005 μm and 0.125±0.016 fl, respectively, for the central 5×5 array of 135×135 μm^2. Thus in these areas, to which the experiments were restricted, the focal volume can be assumed constant.

4.2 RICS experiments

RICS experiments were done to verify the guidelines given in Eq. (4) and by Digman et al. [17]. The correlation curves were plotted and fitted for at least the first 30 pixel shifts along the line in x direction, always without $\xi = 0$ because of the strong autocorrelation of the shot noise. Pixel shifts in y direction were not used because the line times are >1 ms and thus much larger than τ_{diff}. Experiments performed with dyes in solution showed that the fitted diffusion coefficient showed some variation with the used scanning velocity. For the same scanning velocity higher sampling yielded better results.

Figure 3 shows an example of a RICS experiment performed in an EGFP-expressing HeLa cell where a 50×50 pixel, 1.5×1.5 μm^2 ROI was chosen in the nucleolus with varying scanning velocities (pixel dwell times) and a constant pixel shift of 30 nm. In the cytoplasm the apparent diffusion coefficient of EGFP is expected to be ~23 μm^2 s^{-1} [36–38]. Due to obstacles presented by the nuclear structure, especially in the nucleolus [31, 39] the resulting apparent diffusion coefficient should be smaller than in the rest of the cell. Although this obstruction effect could be described in principle with anomalous diffusion, we obtained an apparently reduced diffusion coefficient because the signal-to-noise ratio of our measurements did not allow to distinguish anomalous from free diffusion. We chose scanning frequencies resulting in pixel dwell times between 9.4 and 37.3 μs and scanning velocities between 805 and 3198 μm s^{-1}, respectively, complying with the recommended range and covering the value of 980 μm s^{-1} determined with Eq. (4). Table 1 shows that we could obtain

#131566 - $15.00 USD Received 13 Jul 2010; accepted 11 Aug 2010; published 22 Sep 2010

reasonable fit results for every pixel dwell time. However, each data point featured a rather large error most likely

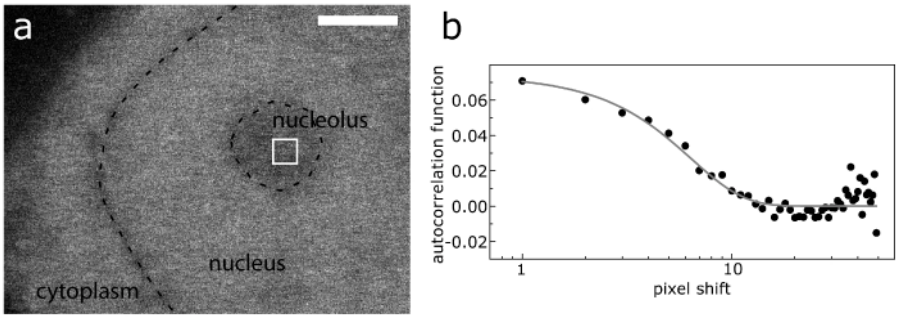

Fig. 3. RICS in a living cell. (a) Detail of a confocal image of a HeLa cell expressing EGFP with a ROI in the nucleolus (white square; 50×50 pixels, 1.5×1.5 μm^2) used for RICS analysis (scale bar 5 μm): (b) autocorrelation function averaged over 7 images acquired at 35 Hz scanning frequency (circles) and fit (line) of Eq. (2) yielding a diffusion coefficent of 23 μm^2 s^{-1}.

Table 1. Diffusion coefficients *D* from RICS and FCS experiments in EGFP-expressing HeLa cells

f_{scan} [Hz][a]	τ_p [μs][b]	v [μm s^{-1}][c]	D [μm^2 s^{-1}]
35	9.4	3198	23 + 39/– 21
20	17.8	1690	27 + 39/– 27
15	24.3	1237	31 + 38/– 29
10	37.3	805	16 + 37/– 15
global/average			24.4 ± 6.7
point FCS[d]			21.9 ± 4.7

[a] scanning frequency
[b] pixel dwell time
[c] scanning velocity
[d] apparent diffusion coefficient using τ_{diff} from an anomalous diffusion fit but the equation for free diffusion

because the ROI was very small. This could be reduced significantly by averaging as well as global analysis over different scanning velocities which led us to the msICS approach where a systematic "scan" of pixel dwell times is employed. It should be noted that both RICS and msICS experiments are less sensitive to saturation effects than FCS because the pixel shift is independent of the optical resolution and both the diffusion coefficient *D* and the focal radius w_0 are independent fit parameters. Indeed w_0 obtained from fits to all RICS and msICS data was ~200 nm, i.e. as large as determined with FCS at the same excitation intensity and ~40% larger than at lower intensities as typically used for FCS experiments (~140 nm). This is in good agreement with the saturation-induced intensity dependence of the focal radius as shown in Fig. 2a.

4.3 msICS experiments with fluorophores in solution

To evaluate the msICS approach we used Alexa488 in aqueous solution (20 nM). The ROI was set to 200×200 pixels (6×6 μm^2) and the fits were carried out either separately for different pixel shifts ($\xi = 1$ and $\xi = 2$, see Fig. 4a) or globally ($\xi = 1,2$ and $\xi = 1\ldots10$, see Fig. 4b). As Table 2 shows, the resulting diffusion coefficients were in good agreement with our expectations and conventional point FCS measurements, see Fig. 4c. Especially the $\xi = 1$ and the $\xi = 2$ correlation functions strongly resembled the point FCS correlation function, featured a comparable signal-to-noise ratio and allowed a good fit. Like in other multifocal FCS implementations, the result is less dependent on aberrations of the PSF.

#131566 - $15.00 USD Received 13 Jul 2010; accepted 11 Aug 2010; published 22 Sep 2010

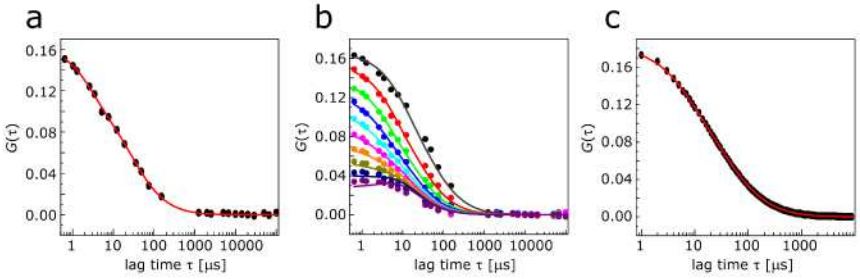

Fig. 4. msICS in solution. (a) msICS, $\xi = 2$, of Alexa488 (20 nM) from a ROI of 200×200 pixels and 6×6 µm^2 (circles) and fit (line) with Eq. (2). (b) msICS, $\xi = 1\ldots10$ (circles, decreasing amplitude with increasing ξ), of the same sample and ROI with global fit (lines). (c) Point FCS of the same sample (circles) and fit (line) with Eq. (7). For fit results see Table 2.

Table 2. Diffusion coefficients D from msICS experiments of Alexa488

pixel shift ξ	D [µm^2 s^{-1}]
1	245 ± 8
2	210 ± 13
1, 2 (global)	220 ± 12
1…10 (global)	235 ± 12
0 (FCS)	210 ± 21

4.4 msICS experiments with HeLa cells expressing EGFP

We tested the applicability of msICS in vivo with HeLa cells expressing EGFP. Figure 5 shows the msICS curves for the pixel shifts $\xi = 1\ldots10$ acquired in a nucleolus and evaluated for a single ROI of 100×100 pixels (3×3 µm^2). It demonstrates how this approach extends the RICS concept: in one dimension (pointing to the right), it shows the msICS curves to given pixel shifts whereas in the other dimension, it represents the RICS correlation functions to given scanning frequencies with the pixel shift contribution at lag times below a lag time of ~200 µs and the line shift contribution above. From a global fit of Eq. (2) to the data, an apparent diffusion coefficient of 10.2 ± 1.7 µm^2 s^{-1} was obtained in agreement with point FCS measurements we performed in these cells and with previous studies based on FCS [31, 37, 39]. After reducing the ROI size at the same position to 50×50 pixels (1.5×1.5 µm^2) the fit produced a rather comparable diffusion coefficient of 12.2 ± 5.1 µm^2 s^{-1}, albeit with a larger error. Thus such a ROI provides usable data with spatial resolution enabling to map diffusion coefficients with ~1 µm sampling. For even smaller ROIs (e.g. 30×30 pixels) the data became too noisy to be evaluated.

To actually allow to fit the data, a correction for slowly mobile or immobile structures had to be applied as described above using various sizes d of the moving average filter, see Eq. (6). For 50×50 pixel ROIs a useful size was in the range of 31-81 pixels, i.e. large enough to leave the diffusional fluctuations unaffected but small enough to actually remove slow or static fluctuations, so that we applied $d = 51$ to all subsequent experiments.

#131566 - $15.00 USD Received 13 Jul 2010; accepted 11 Aug 2010; published 22 Sep 2010

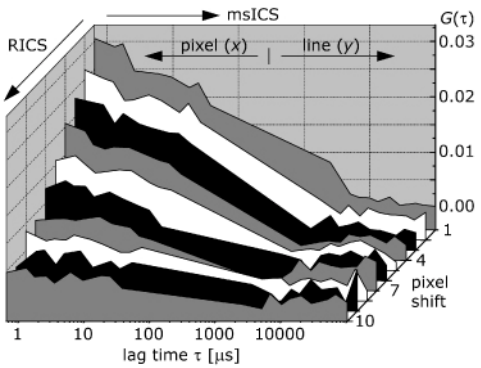

Fig. 5. Two-dimensional graph of the autocorrelation functions of data acquired in the nucleolus of a HeLa cell expressing EGFP (ROI: 100×100 pixels, 3×3 µm^2), plotted over the pixel shift ξ (RICS curves, fixed τ_p) and the pixel dwell time τ_p/line time τ_l (msICS curves, fixed ξ).

4.5 Map of diffusion coefficients

As shown above, msICS should allow to generate maps of the mobility of EGFP in HeLa cells. Figure 6a shows an example of a HeLa cell expressing EGFP, an area of which was divided into 13×15 ROIs (each 50×50 pixels, 1.5×1.5 µm^2) covering 10.5×12.0 µm^2 at two-fold oversampling and including different cellular compartments represented by msICS curves from a nucleolus, the nucleoplasm and the cytoplasm (Fig. 6b). An evaluation as described in the previous section yields a diffusion coefficient for every ROI that can be used for a two-dimensional map, see Fig. 6c for a contour plot representation. It should be noted that there are always data sets that are too noisy to be analyzed. Variations in the mobility of the EGFP molecules represented here by the apparent diffusion coefficient are mainly due to different degrees of obstruction of the diffusion process caused by subcellular structures such as chromatin and associated complexes of different densities in the nucleus and the nucleolus or the endoplasmatic reticulum (ER) in the cytoplasm [31, 39, 40]. From 6 experiments, we could distinguish the apparent diffusion coefficient of 20.4 ± 2.4 µm^2 s^{-1} in the nucleoplasm from 9.5 ± 1.4 µm^2 s^{-1} in the nucleoli.

5. Conclusion

Multiple scan speed intensity correlation spectroscopy (msICS) is a useful tool to measure and map the diffusion of molecules with spatial resolution in living cells. It extends the concept of RICS and benefits likewise from the fact that widely accessible CLSM equipment can be used. In msICS data, the spatial and the temporal information inscribed into a CLSM image are uncoupled but remain subject to a spatio-temporal correlation analysis. In this way, it covers a broad time regime for the processes of interest, for which a priori knowledge is not required, and provides correlation data that are comparable to conventional FCS experiments. It can be applied to subregions of confocal images in a rasterized way so that maps of correlation functions and of the derived parameters can be created.

We could show that spatio-temporal correlation methods are less sensitive to saturation effects on the PSF. We applied RICS to fluorophores in solution and to HeLa cells expressing EGFP and could see that the statistical relevance of the data increased significantly when acquiring images at several scanning velocities (albeit at the cost of the total acquisition time) and employing global fits, resulting in the msICS concept. We devised a strategy to correct for photobleaching and for slow or immobile structures. This allowed us to use msICS to measure the diffusion of fluorophores in solution with a data quality similar to FCS. We also obtained apparent diffusion coefficients of EGFP in HeLa cells in the range of 10-20 µm^2 s^{-1} in good

#131566 - $15.00 USD Received 13 Jul 2010; accepted 11 Aug 2010; published 22 Sep 2010

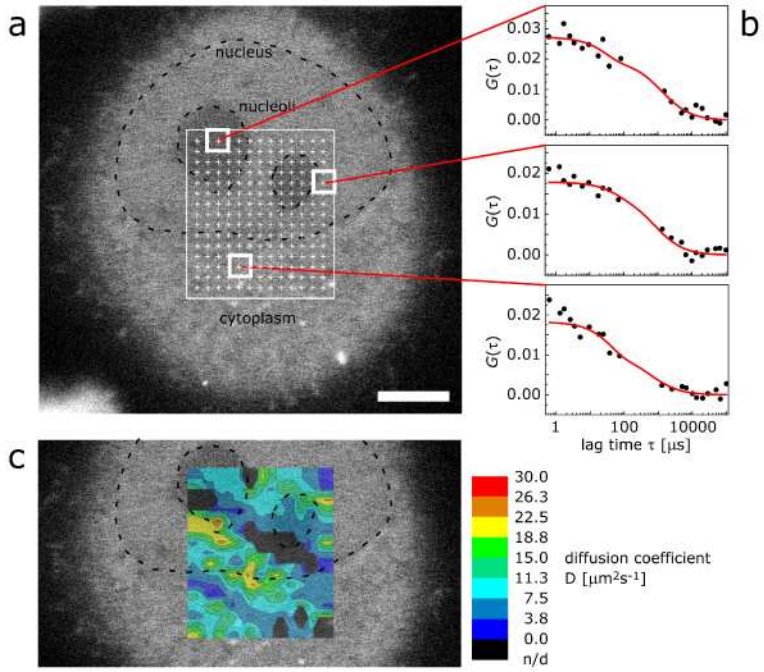

Fig. 6. Map of msICS-derived diffusion coefficients of a HeLa cell expressing EGFP. (a) A 10.5×12.0 µm^2 area covering parts of the cytoplasm, the nucleus and the nucleoli was sampled with 13×15 ROIs (50×50 pixels, 1.5×1.5 µm^2, white squares) that were centered around the white crosses corresponding to two-fold oversampling and used for msICS analysis (scale bar 5 µm). (b) autocorrelation curves ($\xi = 1$, circles) and fits (red lines) of Eq. (2) acquired at positions in a nucleolus, the nucleus and the cytoplasm yielding diffusion coefficients of 8.1, 7.6, and 5.6 µm^2 s^{-1}, respectively. (c) Resulting contour map of diffusion coefficients (black for areas where the correlation analysis failed – n/d, not determined).

agreement with previous results. With a generated map of apparent diffusion coefficients some structural information could be correlated with molecular mobilities with a resolution in the order of 1 µm confirming that especially in the nucleolus of HeLa cells in interphase, the density of the genetic material strongly obstructs the molecular diffusion.

Alternative approaches implement fully sequential acquisition of point FCS measurements by scanning the stage or the beam [39, 41] with comparably high temporal resolution but either limited range of accessible lag times or comparably long total measurement time, or they employ multifocal camera-based setups for parallelized acquisition [42–44] where the measurement time is significantly reduced, however at the cost of time resolution. Our approach bridges the gap between dedicated custom-designed setups and the conventional CLSM with the corresponding raster-scanning scheme as used for msICS ideally in combination with photon-counting detectors. It makes msICS a promising tool to measure and map even more complex diffusion processes with data similar to conventional FCS.

Acknowledgements

This work was supported by the EpiSys project within the BMBF SysTec program. We would like to thank Jessica Kehrer (EMBL) for help with the cell culture, the Advanced Light Microscopy Facility of EMBL for their support, Rolf Borlinghaus and Lioba Kuschel (Leica Microsystems) for fruitful discussions and for providing some of the microsocpy equipment.